Behling, R., Bochow, M., Förster, S., Roessner, S., Kaufmann, H. (2015): Automated GIS-based derivation of urban ecological indicators using hyperspectral remote sensing and height information. - *Ecological Indicators*, *48*, p. 218-234.

DOI: http://doi.org/10.1016/j.ecolind.2014.08.003

Automated GIS-based derivation of urban ecological indicators using hyperspectral remote sensing and height information

Robert Behling[a,*], Mathias Bochow[a,b], Saskia Foerster[a], Sigrid Roessner[a], Hermann Kaufmann[a]

[a]Section 1.4 – Remote Sensing, Helmholtz Centre Potsdam GFZ German Research Centre for Geosciences, Telegrafenberg, 14473 Potsdam, Germany

[b]Animal Ecology I, University of Bayreuth, 95440 Bayreuth, Germany

[*] Corresponding author. Tel.: +493312881766; fax: +493312881192; *E-Mail address:* behling@gfz-potsdam.de (R. Behling)

ABSTRACT

Urban ecological indicators allow the objective and quantitative characterisation of ecological conditions in a spatially continuous way by evaluating the influence of urban surface types with respect to ecological functions and ecosystem services. Although the concept had already been developed in the 1980s, the variety of existing indicators had not been widely applied yet in urban planning practice, because of the high manual mapping effort that is required for spatially differentiated urban surface mapping. This paper presents a new automated remote sensing and GIS-based system for the flexible and user-defined derivation of urban ecological indicators. The system is based on automated surface material mapping using airborne hyperspectral image data and height information. Because the material classes obtained from remote sensing analysis differ in part from the surface types needed for the calculation of urban ecological indicators, they have been transformed into so-called linking categories representing the basis for the automated GIS-based derivation of urban ecological indicators. For this purpose, a computer-based system for flexible indicator derivation has been developed, allowing the user-defined integration of indicators based on the variable determination of mapping units, linking categories and respective weighting factors. Based on a comprehensive review of existing ecological indicators, 14 indicators have been selected and implemented in the system. To demonstrate the potential of the new system, a variety of indicators has been derived for two test sites situated in the German cities of Dresden and Potsdam, using city blocks defined by the municipal authorities as spatial mapping units. The initial mapping of surface materials was automatically performed on the basis of airborne hyperspectral image data acquired by the HyMAP system. The results of subsequent GIS-based indicator calculation were validated using results from field-based reference mapping that had been carried out for selected city blocks situated in both cities. An accuracy assessment for these reference city blocks has revealed mean errors of approximately 4 %, confirming the suitability of the developed automated GIS-based system for flexible and efficient indicator calculation.

Keywords: Urban planning; urban ecological indicators; urban surface materials; remote sensing; hyperspectral; GIS

1. INTRODUCTION

Urban ecological indicators represent quantitative and spatially continuous descriptions of ecological conditions in the urban environment. They belong to the group of urban sustainability indicators that have been developed for evaluating and monitoring economic, social, infrastructural, ecological/environmental and population related aspects

of ongoing urbanisation processes with the goal of supporting urban planning towards more sustainable urban development (Button, 2002; Li et al., 2009; Munier, 2011; Schwarz, 2010).

The urban ecological indicators reflect the widely acknowledged influence of urban surfaces on many ecological functions and ecosystem services, such as groundwater recharge, retention of contaminants, air purification and urban climate regulation (Arlt and Lehmann, 2005; Bolund and Hunhammar, 1999; Eliasson and Svensson, 2003; Gomez-Baggethun and Barton, 2013; Henry and Dicks, 1987; Pickett et al., 2001). They build on the spatially differentiated mapping of urban surface types and represent measures for the fulfilment of ecological functions within predefined spatial mapping units (e.g., city blocks, land parcels or districts). Thus, they allow the quantitative and spatially continuous ecological assessment of urban areas given the availability of urban surface type maps of sufficient thematic and spatial detail.

The concept of surface type-based urban ecological indicators was already introduced for urban planning purposes in Germany in the 1980s and 1990s (Berlekamp and Pranzas, 1986; Krause, 1989; Sandtner, 1998). As a result, a variety of urban ecological indicators was developed including, among others, the *(weighted) imperviousness* (Berlekamp and Pranzas, 1986; Weng, 2012), *vegetation density value* (Krause, 1989, Kumar et al., 2012) and *integrated ecological value* (Heber and Lehmann, 1996). Because the required surface type mapping has been mostly carried out by labour-intensive field surveys and the visual interpretation of aerial photographs (e.g., Cadenasso et al., 2007), the derivation of these indicators has been limited to rather small areas and thus prevented a wider use of ecological indicators in practical urban planning.

To reduce the required manual mapping effort, alternative approaches for the derivation of urban ecological indicators have been developed that do not require the spatially explicit mapping of urban surface types. One of them is the visual estimation of indicator values based on aerial photographs (Schulte et al., 1993), which comprises a high degree of subjectivity and has no potential for automation. The urban structural units (USU) approach (Böhm, 1998; Gill et al., 2008; Haggag and Ayad, 2002; Schiller, 2003) is more sophisticated and based on the assumption that each USU is characterised by a typical composition of urban surface types resulting in USU-specific indicator values. These values are determined for a representative number of mapping units belonging to the same USU by the detailed manual mapping of surface types. In the next step, the derived indicator values are extrapolated to all spatial mapping units belonging to the same USU. This way, large urban areas only have to be mapped in part with high manual effort. However, this approach represents a simplification and neglects the spatial variability of indicator values for mapping units belonging to the same USU (Pauleit and Duhme, 2000). Moreover, it does not yield the potential for automation.

Since the end of the 1980s, the wider availability of digital multispectral satellite imagery, such as LANDSAT-(E)TM and SPOT, has stimulated the investigation of the potential of these data for the automated spatially continuous mapping of urban surface types required for ecological indicator calculation (Cabral, 2007; Gomarasca et

al., 1993; Jat et al., 2008; Lo, 1997; Lu and Weng, 2004). These analyses have been constrained by the limited spectral resolution characterising the broad multi-spectral bands of these satellite systems. They only allow reliable differentiation between non-vegetated and vegetated urban surfaces and thus solely enable the automated derivation of vegetation-focussed urban ecological indicators, such as the *vegetation density value* (e.g., Kumar et al., 2012). However, the potential of these data has also resulted in the development of new ecological indicators assessing the proportion and the spatial distribution of urban vegetation, e.g., *fraction of surrounding vegetation* (Blaschke et al., 2011), *green index* (Schöpfer et al., 2005) and *urban neighbourhood green index* (Gupta et al., 2012).

Because of the limited spectral resolution of the multi-spectral data, the level of thematic detail that can be achieved in mapping urban surface types is not sufficient for the derivation of most urban ecological indicators, especially when the indicators require differentiated mapping of non-vegetated surfaces such as asphalt, concrete, water bound surfaces or bare ground (Banzhaf and Höfer, 2008; Herold et al., 2003). To address these limitations, indirect vegetation-based approaches have been developed for the derivation of such indicators (e.g., *imperviousness*). According to Weng (2012), these approaches either consider impervious surfaces as a complement to the vegetation fraction (e.g., Carlson, 2004; Kim et al., 2006) or they statistically relate vegetation indices derived from remote sensing data to independently mapped *imperviousness* values (e.g., Yuan, 2008). These methods also represent simplifications that neglect the different degrees of surface sealing occurring in non-vegetated areas. Thus, they are also lacking a consequential physical background, which limits their applicability and transferability to other study areas.

Since the 1990s, hyperspectral remote sensing has opened up new opportunities for physically based material mapping due to the continuous acquisition of spectral information by a high number of narrow and adjacent spectral bands (e.g., Goetz, 2009). This high spectral resolution allows the differentiation of distinct material-specific spectral features that cannot be resolved by multispectral imagery (e.g., Heiden et al., 2007; Hepner and Chen, 2001; Herold et al., 2004). Using hyperspectral data in an urban context has enabled the identification of a wider range of urban surface materials, especially in the case of non-vegetated urban surfaces (e.g., Heldens et al., 2011; Roessner et al., 2011). However, exploring the full spectral information content of these data requires specialised automated methods for hyperspectral image analysis (e.g., Fauvel et al., 2008; Franke et al., 2009; Plaza et al., 2009; Roessner et al., 2001; Segl et al., 2003; Tuia and Camps-Valls, 2011). These methods result in a new quality of material mapping and provide valuable input information for the rapidly advancing developments in the GIS-based quantitative characterisation of urban areas. For example, Heiden et al. (2012) has demonstrated the principle suitability of hyperspectral material mapping in combination with height information for the derivation of selected urban ecological indicators (e.g., *imperviousness*, *building density*) for the city of Munich.

The new quality of remote sensing-based urban surface material mapping, which can be achieved using hyperspectral imagery, has motivated the development of an automated system for the efficient and flexible derivation of urban ecological indicators that builds on automated hyperspectral material mapping and GIS-based

analysis. This new system enables the flexible and automated calculation of ecological indicators including the user-defined implementation of new indicators and variable spatial mapping units. Methodological developments comprise the implementation of a wide range of ecological indicators that have been developed for urban ecological planning in Germany. The potential of the developed system is exemplarily demonstrated for two test sites within the German cities of Dresden and Potsdam by deriving a variety of urban ecological indicators for these test sites. The obtained indicator values are validated by field mapping-based accuracy assessment and by comparing them with results derived by state-of-the-art methods used in urban planning practice in Germany.

2. STUDY AREAS, DATA AND PRE-PROCESSING

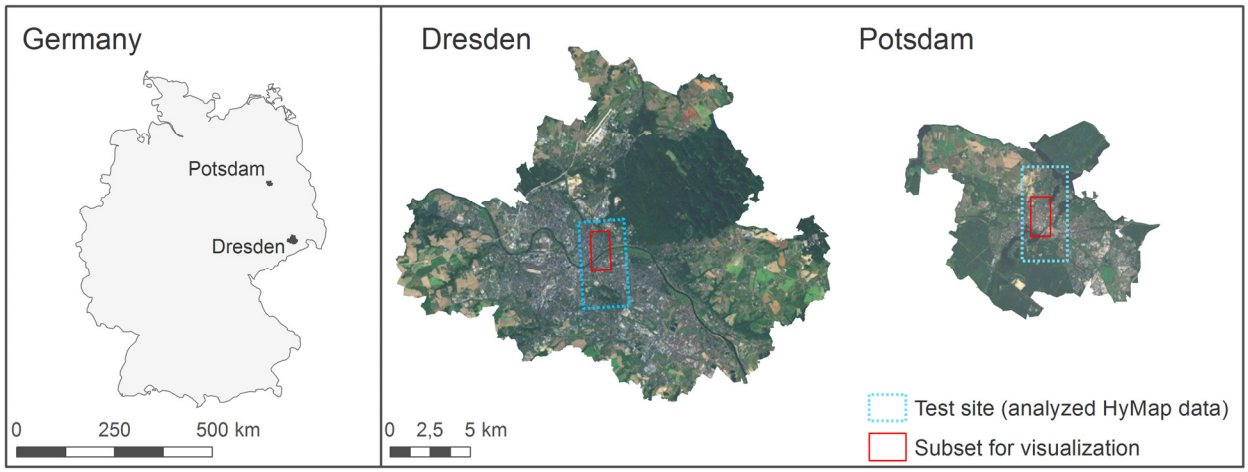

Figure 1: Overview of study areas. Location of test sites within the city landscape and location of subsets used for visualisation purposes within this paper.

2.1 Study areas

The German cities of Dresden and Potsdam (Figure 1) were selected as study areas because they both represent typical large German cities, serving as the capitals of the federal states of Saxony and Brandenburg. Due to their specific historic development, they differ in part in their building structures while also showing many similarities relevant to remote sensing analysis, such as commonly used roof and surface materials. Thus, the consideration of two different cities increases the variability of surface representations within the analysed imagery caused by varying terrestrial conditions and differences in the airborne imaging processes. This way, the initial evaluation of the robustness of the developed approach can be performed as a first step towards achieving broader methodological transferability.

Within the city of Dresden, with its more than 500,000 inhabitants, a 4.5 km by 2 km test site was chosen covering a comprehensive variety of urban structures including densely built-up areas in the north and large vegetated areas of the landscape park ‘Grosser Garten’ in the south. For the city of Potsdam, with a population of approx. 150,000 inhabitants, a 5.8 by 2.8 km test site was chosen that also contains various urban structural elements ranging from the densely built-up city centre to low-density housing such as multi-storey blocks and single-family houses.

2.2 Hyperspectral database

The developed system builds on hyperspectral remote sensing data as the main source of spatial information for the automated derivation of urban ecological indicators. These data resolve small-scale material-specific spectral features – such as the spectral decrease of the polyethylene spectrum at 1700 nm and 2200 nm or the absorption bands (local minima) of the bitumen and concrete spectra at 2200 nm and 2300 nm, respectively, in Figure 2 – which are determined by the chemical composition of the materials (Heiden et al., 2007; van der Meer and de Jong, 2001). These spectral features opens up the possibility for the differentiation and identification of urban surface materials such as asphalt, concrete, gravel, fired clay, aluminium, polyethylene, and PVC (e.g., Heiden et al., 2007; Hepner and Chen, 2001; Herold et al., 2004) based on their spectral reflectance characteristics.

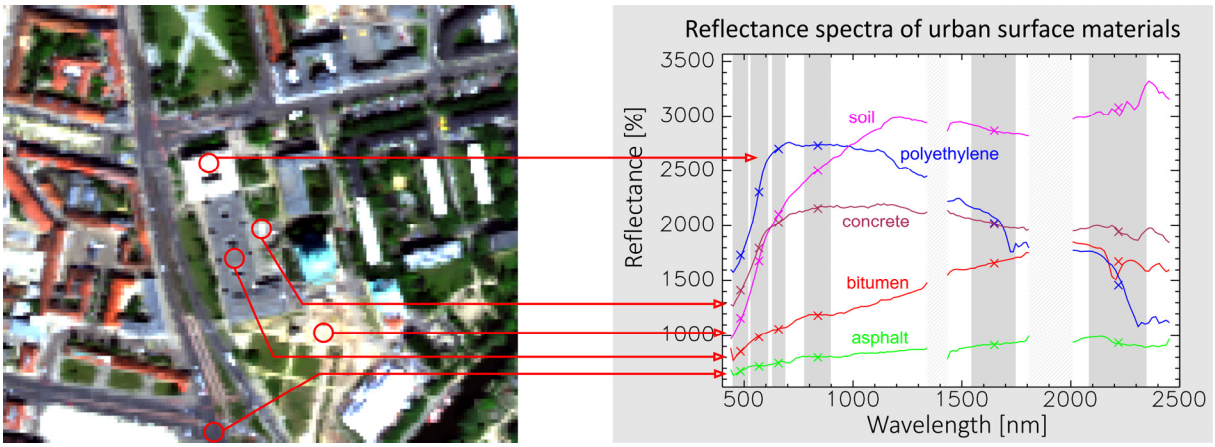

Figure 2: Reflectance spectra of selected urban surface materials recorded by the HyMap sensor. The cross symbols indicate the reflectance values as they would be recorded by Landsat TM5 spectral bands depicted by the grey bars. The gaps in the spectra near 1400 nm and 1900 nm indicate wavelength ranges where atmospheric absorption inhibits spectral measurements.

2.2.1 Spectral inventory of urban surface materials

Detailed spectral knowledge about urban surface materials is stored in spectral libraries in the form of spectral reflectance signatures (also called spectra). In hyperspectral remote sensing these spectra serve as important input information for pre-processing and automated classification procedures. For the purpose of area-wide classification, these spectral libraries have to contain spectra of each surface material occurring in the analysed image data to obtain a spatially complete classification. The spectral libraries used in this study have been established during the last 10 years based on field and imaging spectroscopy for various test sites in the German cities of Berlin, Dresden, Munich and Potsdam. The majority of spectra (approximately 60,000) have been identified interactively in the hyperspectral image database. The surface materials contained in these spectral libraries are summarised in Table 1.

Table 1: Overview of urban surface materials contained in the comprehensive spectral library

	Urban surface materials
Buildings (roofs)	Red clay tiles (new), red clay tiles (old), auburn clay tiles, grey clay tiles, red concrete tiles, aluminium, zinc, copper, steel with protective coating, metal with four different coating colours, PVC, polyethylene, Plexiglas, glass, greenhouses, bitumen roof sheeting (bright/dark/red), tar-paper (obsolete), schist, green roofs, two types of gravel and eight spectrally unique but unknown materials
Artificial open spaces	Three types of concrete, asphalt, tartan track, synthetic turf, polyethylene pavement panels cobblestone pavement, concrete, red/dark/bright/grey loose chippings, red concrete pavement stones, red clay-baked pavement stones, red cinder (tennis court or running track), railway tracks
Bare ground	Siliceous sand, coarse construction sand, soil
Water	River, pond, lake, pool
Vegetation	Deciduous trees, coniferous trees, lawn, meadow, dry grass, tilled field, untilled field, fallow
Other	Shadowed vegetated and non-vegetated areas

2.2.2 Hyperspectral image data

The hyperspectral image data used in this study were acquired by the digital airborne imaging spectrometer HyMap– a whiskbroom scanner that records image data in 126 spectral bands throughout the visible (VIS), near infrared (NIR) and shortwave infrared (SWIR I + II) wavelength ranges (Cocks et al., 1998). Image data were recorded for a total of 11 flight lines providing multi-temporal coverage of test sites in the German cities of Berlin, Dresden, Munich and Potsdam. The spatial resolutions range from 3 to 6 m. All images were used for the establishment of a comprehensive urban spectral library as described above. Automated urban material mapping (Section 3.2) was performed for the city of Potsdam based on the flight line acquired at the 19 May 1999 and for the city of Dresden based on the flight line acquired at 7 July 2004.

The automated thematic analysis of hyperspectral image data requires pre-processing, which includes radiometric, atmospheric and geometric correction (Richter and Schläpfer, 2002; Schläpfer and Richter, 2002). Radiometric correction primarily consists of the conversion of raw digital numbers measured at sensors to physical unit radiance and has been performed by the sensor operating company. The atmospheric correction of the HyMap data was carried out using a MODTRAN-based parametric approach including a digital elevation model (DEM) as supplementary information, followed by a field spectra-based Empirical Line Correction to eliminate remaining spectral spikes. Geometric correction was performed using an in-house developed parametric geocoding approach based on in-flight recorded exterior orientation parameters, a DEM and ground control points. The resulting RMS errors amount to a maximum of one pixel and thus allow an accurate overlay of the image data with other spatial input data within a GIS system.

2.3 Height information

Height information has been used in different processing steps of the developed system for the derivation of urban ecological indicators. Digital terrain models (DTM) representing the topographic heights at the Earth's surface are required for geometric and atmospheric correction during the pre-processing of the hyperspectral image data. For the city of Potsdam, a DTM with a grid size of 25 m was provided by the state survey office. For the city of Dresden, the DTM was generated based on a last pulse LiDAR digital surface model (DSM) of 1 m horizontal resolution using multiple filtering techniques (Bochow, 2010; Bochow et al., 2010). The initial LiDAR DSM was acquired by the TopScan GmbH during the leaf-off period in December 2002 and provided by the municipalities of Dresden.

Height information has also been used in the form of a mask of high objects to distinguish between surface types that represent different categories in the context of urban ecological indicator derivation and are covered by spectrally similar surface materials (mainly differentiation between open spaces and buildings covered by the same material, such as bitumen and concrete). For the city of Dresden, such a mask of high objects has been derived from a normalised digital surface model (nDSM), which has been generated by subtracting the LiDAR-based DTM from the initial LiDAR DSM containing the height information of the uppermost surfaces, including roof and vegetation tops. Thus, the resulting nDSM represents object height information for buildings and vegetation. The final mask of high objects has been generated from this nDSM by applying a height threshold of 1.8 m representing the minimum height of a building. This threshold is also higher than the Absolute Linear Error 90 of the nDSM to exclude false positives.

For the city of Potsdam, the mask of high objects has been derived from a vector layer containing buildings with attributed height information that was provided by the state survey office of Brandenburg. Thus, for Potsdam the mask of high objects solely includes buildings representing the main source of ambiguities in hyperspectral material mapping. In contrast, vegetation of different height (e.g., trees/bushes and meadow/lawn) is robustly distinguishable based on the different spectral characteristics of these vegetation types (Heiden, 2007). This situation has been considered in the development of the automated processing system for urban material mapping (Section 3.2) by implementing the mask of high objects as a spatial information source, which can be enabled optionally for the different surface types.

2.4 City blocks as basic mapping units

For urban planning purposes, cities are divided into spatial units representing different aggregation levels, such as land parcels, city blocks and districts, whereas city blocks are the spatial units most commonly used in urban planning and urban design (Carmona et al., 2003; Komossa et al., 2005; Towers, 2005). In this study, city blocks also serve as spatial mapping units for the derivation of urban ecological indicators. These city blocks (Figure 3) were provided in the form of vector data by the municipal authorities of the cities of Dresden and Potsdam. For the city of Dresden, they consist of an urban structural unit data set, and for the city of Potsdam they are part of the Authoritative Topographic Cartographic Information System (ATKIS). The urban structural unit data set of the city of Dresden also

contains the ecological indicator *imperviousness* (IMP) as one of the attributes for each city block. These IMP values represent visual estimates that have been determined in 20 % steps based on aerial photographs. In this study, these estimates have been used for the evaluation of results obtained by the developed automated approach in comparison to a state-of-the-art method that is used by the municipal authorities of Dresden (Section 4.3)

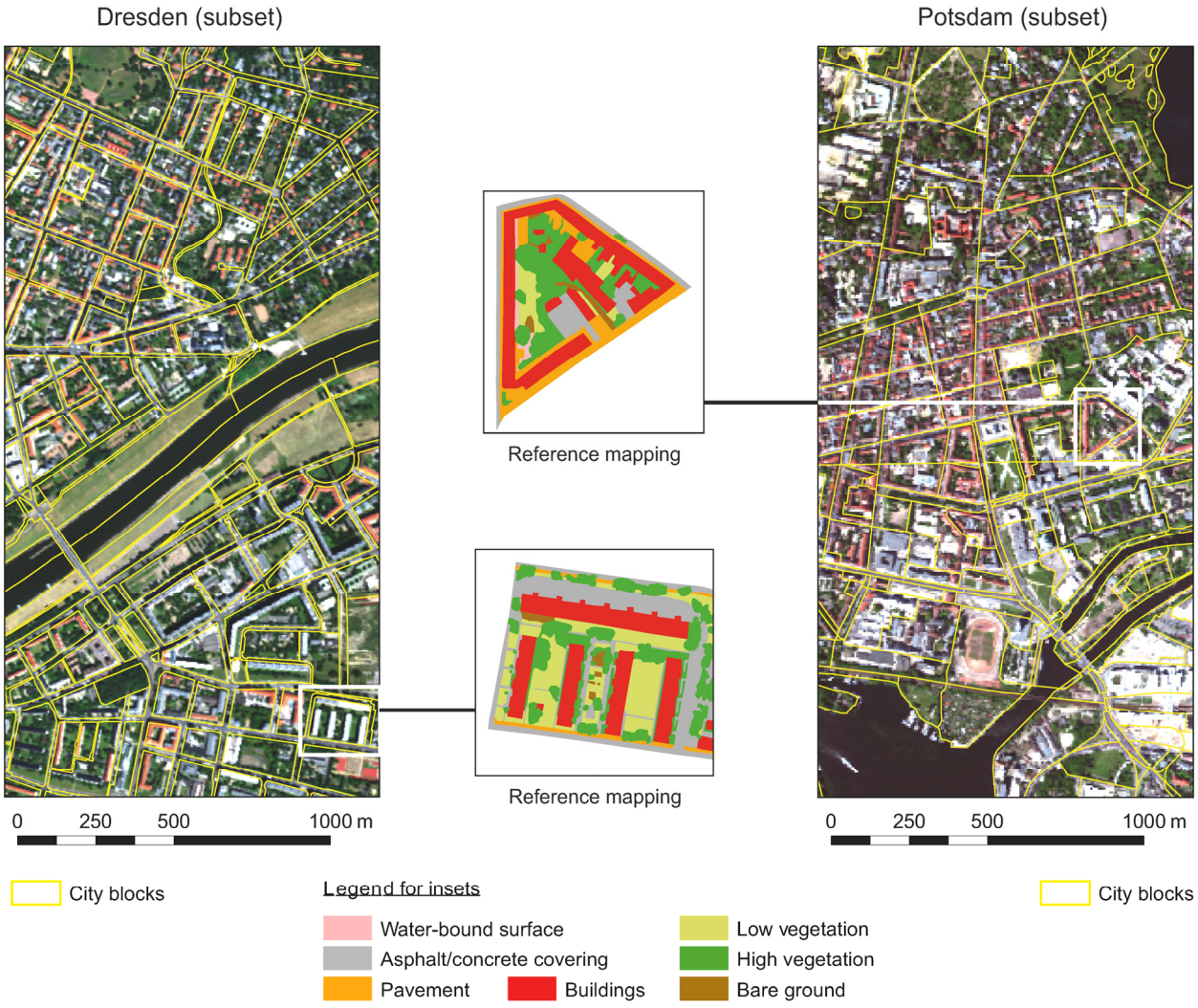

Figure 3: Subset of test sites in Dresden (left) and Potsdam (right) depicted as true colour composites of the used hyperspectral image data overlaid by city blocks (yellow lines). Insets: Exemplary reference city blocks.

2.5 Reference mapping

For accuracy assessment, the material coverage of individual city blocks has been digitised manually on-screen using orthorectified aerial photographs of 0.25 m resolution acquired in 2004 and 2005 for Dresden and in 1998 for Potsdam. Additional field investigations were carried out to resolve remaining ambiguities. As a result, 22 built-up city blocks were mapped situated in both cities. Figure 3 depicts exemplary city blocks including a legend showing

the level of thematic detail contained in the reference mapping. These reference blocks comprise urban structural units that are common for Mid-European cities and contain a comprehensive selection of urban surface materials.

3. REMOTE SENSING AND GIS APPROACH FOR THE AUTOMATED DERIVATION OF URBAN ECOLOGICAL INDICATORS

Section 3.1 introduces the principles of ecological indicator calculation and gives an overview of existing indicators and the surface types that are required for their derivation. Section 3.2 presents the hyperspectral classification approach, including the results of the automated identification of urban surface materials. Section 3.3 describes the adaptation of these results to the requirements of ecological indicator derivation and presents the GIS-based system that has been developed for the flexible, user-defined and spatially continuous calculation of urban ecological indicators.

3.1 Urban ecological indicators

Thematically, urban ecological indicators represent varying degrees of urban surface differentiation. The main subdivision consists of the differentiation between vegetated non-sealed surfaces with positive ecological influence on the urban environment and non-vegetated impervious surfaces with negative ecological influence (Gao et al., 2012; Gómez et al., 2011; Li et al., 2012; Weng et al., 2011). To allow a more detailed ecological characterisation, these two groups are further subdivided into surface types with different influences on specific ecological functions/services. These surface types include impervious surfaces (e.g., concrete and asphalt), water-bound surfaces (e.g., loose chippings, cinder), bare ground (e.g., soil, sand) and different categories of vegetation (e.g., lawns, meadows, bushes, trees).

Based on the differentiated assessment of surface types, urban ecological indicators of different complexity levels have been developed. The indicators can be divided into three types: weighted parameters (wP), non-weighted parameters (nwP), and integrative indicators (iI). While the parameters evaluate individual ecological compartments, integrative indicators allow ecological assessment across compartments by combining and weighing various parameters. Table 2 shows a selection of 19 indicators and their required input information, differentiated in thematic urban surface types and additional non-surface-related information. This selection comprises indicators of each indicator type and for different ecological compartments. All of them allow the spatially continuous ecological characterisation of urban environments and are either in practical use or have been widely discussed in the literature. Most of these indicators have been developed for urban planning purposes in Germany since the beginning of the 1990s, taking into account an increasing need for considering ecological aspects in urban planning. Therefore, the table also contains the German abbreviations of the indicators and the references to the original sources of publication.

The general mathematical principle of the calculation of urban ecological indicators is shown in Equation 1. The indicator value results from the multiplication of the areas of the urban surface types within the spatial mapping unit and the corresponding weighting factors and is finally normalised by the total area of the spatial mapping unit. The

weighting factors depend on the objective of the indicator and are mostly empirically determined according to the impact of the specific urban surface type on the specific ecological compartment.

$$\text{indicator value} = \frac{\sum_{i}^{n}(\text{area of urban surface type i} \times \text{weighting factor i})}{\text{Area of the spatial mapping unit}} \quad (1)$$

Apart from this, some urban ecological indicators, particularly the integrative ones, require additional information, such as the height of vegetation and buildings, the number of floors in the buildings, the presence of roof and facade greening, the spatial air temperature distribution, sewerage connection, type of subsurface or the type and percentage of paving joints within semi-impervious surfaces (Table 2).

All of the surface types listed in Table 2 have the potential to be automatically identified by means of remote sensing. It has already been shown that some of the additional information contained in Table 2 can be automatically extracted from remote sensing data. Examples are green roofs derivable from optical images and digital elevation models (Roessner et al., 2011) and height information of vegetation and buildings derivable from digital elevation models (e.g., Hecht et al., 2008; Kraus and Pfeifer, 2001; Mayer, 2000). As a result, 14 indicators (highlighted in grey in Table 2) have been evaluated as being derivable in principle by remote sensing analysis and are further analysed within this paper.

Table 2: Overview of urban ecological indicators and required information for their derivation (highlighted grey: indicators derivable by remote sensing)

English abbreviation of indicator	Full name of indicator [indicator type: nwP = non-weighted parameter, wP = weighted parameter, il = integrative indicator]	German abbreviation of indicator	Surface types (Artificial | Natural)													Additional information										Reference	Ecological compartment
			Buildings	Asphalt/concrete	Slab paving	Paved stone surface	Water-bound surface	Grass paver	Artificial water	Natural water	Bare ground	High vegetation	Mid-height vegetation	Low vegetation	Vegetation height [m]	Building height [m]	Number of floors	Green roofs	Facade greening	Air temperature	Sewerage connection	Perc. and No. of joints	Type of subsurface		
IMP	Imperviousness [nwP]	VSG	o																						a	Soil
wIMP	Weighted imperviousness [wP]	gVSG	●	●	o		●																		b	
SFV	Soil function value [wP/il]	BFZ	●	●	●	⊙	o			o								●				●	●		c	
OSV	Open space value [nwP]	FFZ	●																						d	
OSIMP	Open space imperviousness [nwP]	FFVSG	o																						d	
wOSIMP	Weighted open space imperviousness [wP]	gFFVSG		●	o		●																		d	
RC	Runoff coefficient [wP]	ABW	●	●	●	●	●	●																	e	Water
IV	Infiltration value [nwP]	IFZ										o													d	
VDV	Vegetation density value [nwP]	VFZ											o												f	Vegetation
VCV	Vegetation coverage value [nwP]	VDG												●											d	
CCV	Canopy cover value [nwP]	ÜFZ										●													d	
VVV	Vegetation volume value [wP]	GVZ										●	●	●	●										g	
BD	Building density [nwP]	GRZ	●																						h	Built structure
FAR	Floor area ratio [nwP]	GFZ	●														●								h	
BV	Building volume [nwP]	BMZ	●													●									d	
IEV	Integrated ecological value [il]	ÖKO-Wert	●	●	o		o		⊙	●	●	●	●	●				●							i	Multiple compartments
CEH	Climatic-ecological-(air-)hygienic value [il]	KÖH-Wert	●	o					o		●	●	⊙	●		●		●	●						k	
CEP	Climatic-ecological-pedological value [il]	KÖP-Wert	●	●	⊙	⊙	●	●	⊙	⊙		⊙	●	⊙	●		●	●		●		●	●		l	
BAF	Biotope area factor [il]	BFF	●	●	o			●				o						●	●		●		●		m	

Explanation of symbols: ● required; ⊙ required in more detail; o required in less detail

References: [a] Berlekamp and Pranzas, 1986; Weng, 2012. [b] Berlekamp and Pranzas, 1992; Heiden et al., 2012. [c] Pohl, 1991; Schulze et al., 1984. [d] Krause, 1989. [e] Haid and Treter, 2004; Illgen, 2000. [f] Krause, 1989; Kumar et al., 2012. [g] Hecht et al., 2008; Pohl, 1991; Schulze et al., 1984. [h] Frick, 2006. [i] Arlt and Lehmann, 2005; Heber and Lehmann, 1996. [k] Schulz, 1982. [l] Rose, 1991. [m] Bötticher and Fisch, 1988; Lakes and Kim, 2012.

3.2 Hyperspectral material mapping

Automated urban material mapping using hyperspectral imagery requires approaches that are capable of fully exploiting the spectral information content of these data. Furthermore, such approaches need to be able to handle a large number of possible surface materials, including their spectral variations and a high percentage of mixed pixels in the image data due to the dominance of heterogeneous and small-sized structures. These requirements have formed the basis for the development of a multi-step hyperspectral processing system for urban material mapping (Roessner et al., 2001, 2011; Segl et al., 2003). The processing scheme of this system is depicted in Figure 4. It comprises standard hyperspectral image analysis techniques that have been combined, modified and extended to meet the special needs of the urban environment.

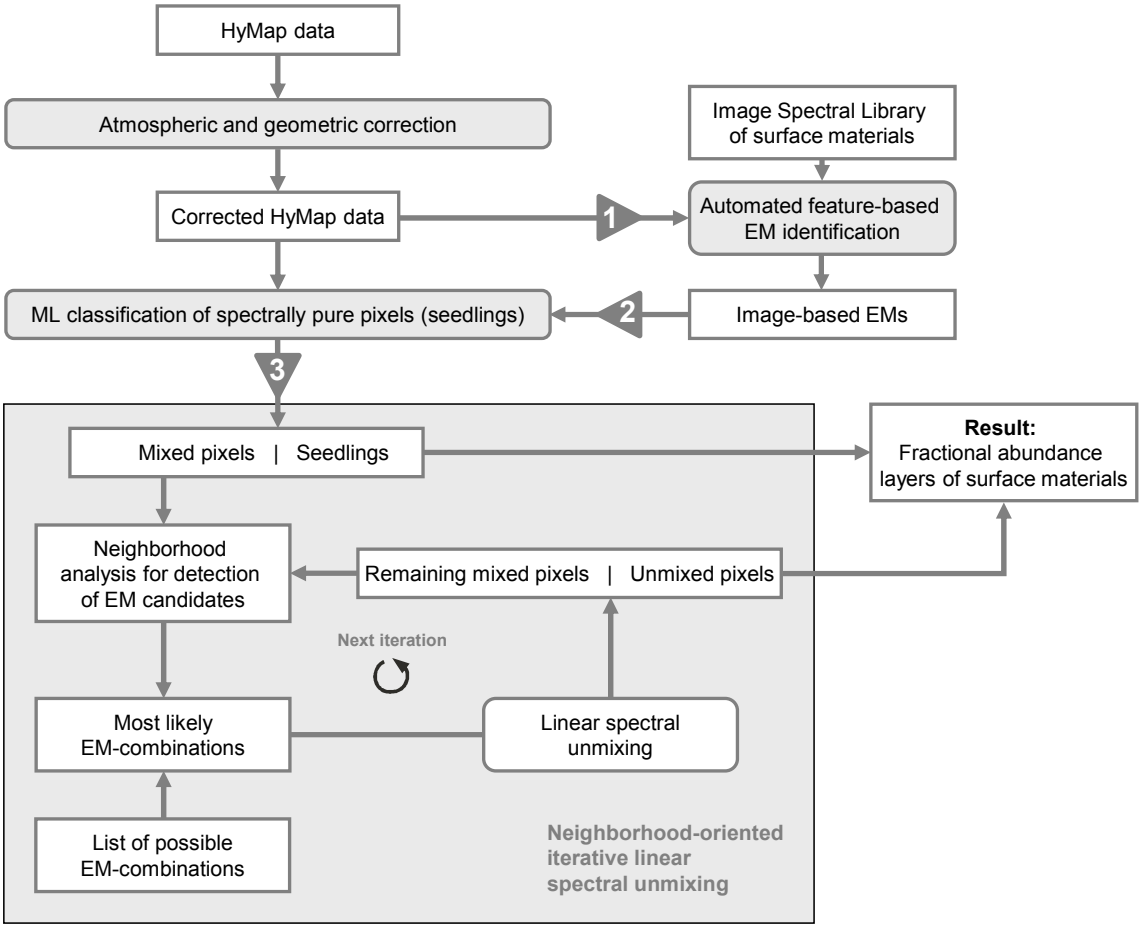

Figure 4: Automated multi-step processing system for urban material mapping. ML = maximum likelihood, EM = endmember

The developed system builds on already pre-processed hyperspectral remote sensing data (Section 2.2) and is described in detail in Roessner et al. (2011). The system has reached a high degree of automation and consists of three major steps. First, endmember (EM) identification is carried out using an automated spectral-feature-based approach (Figure 4, No. 1). Such EMs are represented by distinct spectral signatures or bundles of signatures (Bateson et al., 2000; Theseira et al., 2003) that characterise the surface materials of interest. For automated EM extraction, the existing comprehensive urban spectral libraries (Section 2.2) have been used to build a classifier that enables supervised EM detection. For this purpose, a pairwise Maximum Likelihood classifier has been developed to achieve a class-specific dimensionality reduction. Once the classifier has been established, it can be

applied to any atmospherically corrected hyperspectral dataset to identify the specific EM, reducing the effort for collecting ground truth information and facilitating the transferability of the approach.

The second processing step aims at the optimal separation between pure and mixed pixels, including the identification of the respective surface materials for the spectrally pure pixels based on a Maximum-Likelihood classification (Figure 4, No. 2). In this context, pure pixels are defined as pixels covered by a single surface material. In the case of mixed pixels, two or more surface materials are present within one pixel. The already identified image EM pixels represent the starting points of this separation. They comprise only a small percentage of all image pixels and are further subdivided into representative Gaussian distributed subclasses to accommodate the high spectral variability of urban surface materials in the hyperspectral image data. These subclasses serve as training information for the parameterisation of a Maximum Likelihood classifier for pure pixels and also allow the calculation of class specific Mahalanobis distance thresholds to exclude mixed pixels. The combined identification results of the first and second processing steps represent the total number of spectrally pure pixels.

In the third processing step (Figure 4, No. 3) previously identified pure pixels serve as seedling pixels for analysing the remaining mixed pixels by neighbourhood-oriented iterative linear spectral unmixing (Roessner et al., 2001). The high spectral dimensionality of hyperspectral image data allows the application of linear spectral mixture models, resulting in the estimation of fractional abundances for each EM class within one pixel. However, the application of mixture models consisting of a high number of spectrally similar EMs is not feasible; thus, methods for the individual determination of per-pixel mixture models have been developed (Dennison and Roberts, 2003; Roessner et al., 2001). The developed approach applies iterative spatial optimisation strategies to find a suitable per-pixel mixture model incorporating the previously identified pure pixels and the EM information of previously unmixed pixels. This way, the iterative unmixing procedure leads to the spatial growing of the unmixing results around seedling pixels until all image pixels are processed.

The developed approach also includes the possibility of integrating object height information in the form of a mask of high objects (Section 2.3) in steps 1, 2, and 3 (Figure 4) to distinguish between surface types that are relevant for ecological indicator calculation and have similar spectral characteristics. This way, confusion between open spaces, buildings and different vegetation types can be reduced in the automated classification and unmixing process.

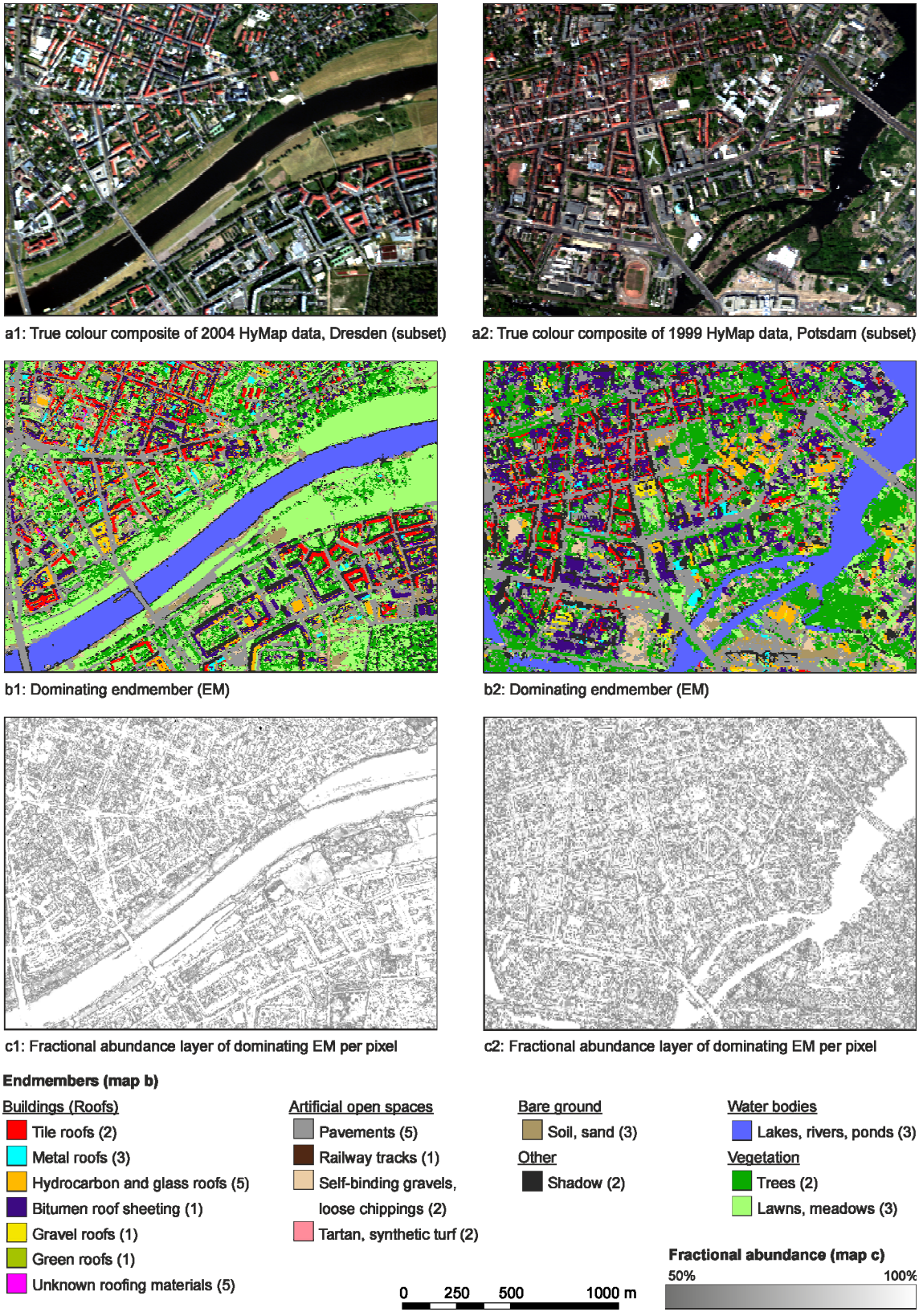

Figure 5: Exemplary results of neighbourhood-oriented iterative linear spectral unmixing for a subset area in the city of Dresden (left) and Potsdam (right). The number in brackets indicates the number of surface materials (Table 1) aggregated into the respective mapping categories.

The result of the automated multi-step processing system for urban material mapping consists of one fractional abundance layer per EM (surface material) that stores the proportional coverage of the respective EM for each pixel. In Figure 5, the urban material mapping results are depicted in an exemplary way for 2 km by 1.3 km subsets of the city centres of Dresden and Potsdam. For the classification-like representation of the results, the dominating EM has been derived for each pixel (Figure 5b1 and b2). For visualisation purposes, the classified surface materials were further aggregated into the material categories contained in the legend of Figure 5, whereas the number in brackets indicates the original number of classified surface material variations. These mapping results are complemented by a greyscale image depicting the fraction of the dominating EM ranging between 50 and 100 % (Figure 5c1 and c2). Areas dominated by small-sized objects are depicted in various shades of grey indicating a high fraction of mixed pixels. These areas can be clearly distinguished from areas characterised by large homogeneous objects depicted in white, such as rivers, meadows, wide streets and large buildings. In the case of low fractional abundances for the dominating EM, the material coverage of the second EM provides valuable information allowing the analysis of the occurrence of surface materials at a sub-pixel level. The obtained material classes that have been automatically mapped on a pixel basis form the input information for the subsequent derivation of urban ecological indicators.

3.3 GIS-based derivation of urban ecological indicators

To automatically derive urban ecological indicators, a flexible GIS-based system has been developed (Figure 6) that has been combined with a graphical user interface (GUI) to enable the interactive determination of ecological indicators and mapping units. The system allows the direct and spatially continuous calculation of a variety of ecological indicators based on the fractional abundances of urban surface material classes resulting from hyperspectral remote sensing (Section 3.2).

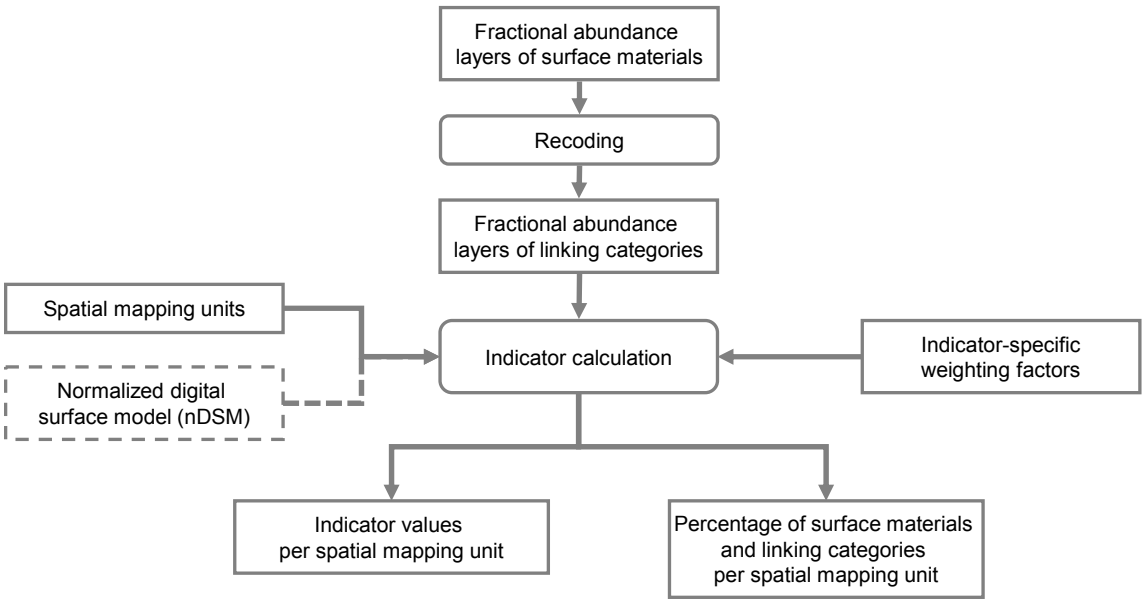

Figure 6: GIS-based system for automated indicator calculation based on hyperspectral material mapping and height information. The incorporation of height information in the form of nDSM data is optional (depicted by dashed box) and can be enabled for selected indicators.

The surface material categories derived from the automated classification of hyperspectral remote sensing data (Section 3.2) differ from the thematic classification of the urban surface types that are used in the calculation of urban ecological indicators (Section 3.1). Thus, the remote sensing-based categories and the surface types need to be transformed into common denominator categories that can then be used for automated remote sensing-based indicator calculation. For this purpose, so-called linking categories have been introduced (Figure 7). Table 3 gives an overview of the surface types required for the calculation of the 14 selected indicators (Table 2), the related surface materials derived from hyperspectral remote sensing (Table 1) and the respective linking categories used for automated GIS-based indicator calculation. The surface material classes have mainly been transformed into the linking categories by thematic matching, aggregation and merging summarised as the recoding step in Figure 6. Table 3 shows that the majority of surface types can be derived from the remotely sensed surface materials by thematic aggregation, such as the linking category 'building' comprising 35 different roof materials, which have been identified in the process of automated hyperspectral image analysis.

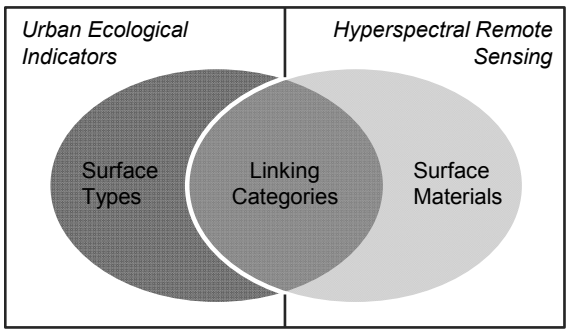

Figure 7: Link between urban ecological indicator derivation and hyperspectral remote sensing.

Only with three indicators – *runoff coefficient* (RC), *vegetation volume value* (VVV) and *integrated ecological value* (IEV) – has such a transformation not been fully possible, because the automatically derived hyperspectral material classes could not be directly linked to all of the surface types needed for the calculation of these indicators. To enable their automated remote sensing-based derivation, slight modifications have been applied to the original indicators. In the case of the linking category 'pavement', three different material classes of pavement derived from hyperspectral remote sensing could not be linked to the two surface types 'slab paving' and 'paved stone surface' (Table 3), differing by their stone size. To overcome this problem, both categories – surface types and surface materials – have been aggregated into one comprehensive linking category 'pavement'. However, this modification only has a subordinate influence on the resulting indicator values and solely affects the indicator RC.

Furthermore, the surface type 'mid-height vegetation' (e.g., bushes, shrubs) could not be distinguished from low and high vegetation in the process of automated hyperspectral material mapping, because the available nDSM (Section 2.3) is not sufficient to adequately differentiate between these three types of vegetation. Reasons include the nature of the last pulse LiDAR data used and the acquisition date in December 2002 occurring outside of the growing season. Nevertheless, it has been possible to reliably differentiate between the surface types 'low vegetation' and 'high vegetation', only leaving the need for omitting the surface type 'mid-height vegetation' from the list of linking categories. Another surface type that could not be identified from

hyperspectral imagery is 'grass paver'. Therefore, the calculation of the three affected indicators (RC, VVV and IEV) has been slightly modified. Overall, 11 out of the 14 implemented indicators can be calculated without any modifications based on the hyperspectral mapping results.

Table 3: Linking categories between remotely sensed surface materials and relevant indicator surface types relevant for indicators.

Surface types (used for urban ecological indicator calculation)		Surface materials (derived from hyperspectral remote sensing)	Linking categories (used for RS/GIS-based indicator calculation)
Artificial	Buildings	35 roof materials (e.g., concrete tiles, clay tiles, bitumen)	Building
	Green roofs	1 (green roofs)	Green roofs
	Asphalt/concrete covering	7 (e.g., asphalt, concrete, tartan)	Asphalt/concrete covering
	Slab paving	3 (cobblestone, concrete and clay-baked pavement stones)	Pavement
	Paved stone surface		
	Water-bound surface	5 (loose chippings, cinder)	Water-bound surface
	Grass paver	---	---
	Pool	1 (pool)	Pool
	Pond	1 (pond)	Pond
	---	Shadow on non-vegetated surfaces	Shadow on non-vegetated surfaces
Natural	Bare ground	3 (soil, siliceous sand)	Bare ground
	Low vegetation	4 (lawn, meadow)	Low vegetation
	Mid-height vegetation	---	---
	High vegetation	2 (deciduous, coniferous)	High vegetation
	Natural water	2 (river, lake)	Natural water
	---	Shadow on vegetated surfaces	Shadow on vegetated surfaces

As described in Section 3.1 and shown in Equation 1, the calculation of urban ecological indicators includes the introduction of indicator-specific weighting factors that characterise the surface types according to the evaluation objectives of the respective indicator. To apply this concept, these weighting factors have been determined for all of the newly established linking categories (Table 4, Figure 8). They have been mostly taken from the publications describing the original indicators (Table 2). When the weighting factors were missing, they were added from other publications including, among others, empirical studies on the infiltration capacity and flow rates (Bunzel, 1992; Din, 1995; Illgen, 2000).

In this context, the two shadow categories listed at the end of Table 4 represent a special case for the determination of weighting factors, because they comprise multiple linking categories; therefore, no distinct weighting factor can be assigned. The results from hyperspectral material mapping allow the discrimination of vegetated and non-vegetated shadowed areas (Table 1). In the urban areas that have been analysed in this study, shadows are mostly caused by buildings or high vegetation and cast over open spaces. Therefore, it can be assumed that shadowed vegetated surfaces most likely belong to the category of low vegetation and thus the respective weighting factor can be assigned to them. In the case of non-vegetated shadowed surfaces, a variety of linking categories - asphalt/concrete, pavement, water-bound surfaces and bare ground – have to be taken into account to derive a weighting factor that can be assigned to non-vegetated shadowed surfaces. For this purpose, the relative areal coverage has been calculated within the analysed test site for each of the four above mentioned non-vegetated linking categories. In the second step, the obtained percentage values have been multiplied by the weighting factors of the respective linking categories and averaged to obtain the area-weighted average for each indicator and test site. The resulting indicator-specific weighting factors for non-vegetated shadowed surfaces are shown in Table 4. This way, the developed approximation approach allows the calculation of ecological

indicators even in cases of shadowed surfaces, which represent a common problem in remote sensing analysis and might cover significant parts of urban areas depending on the dominating building structures.

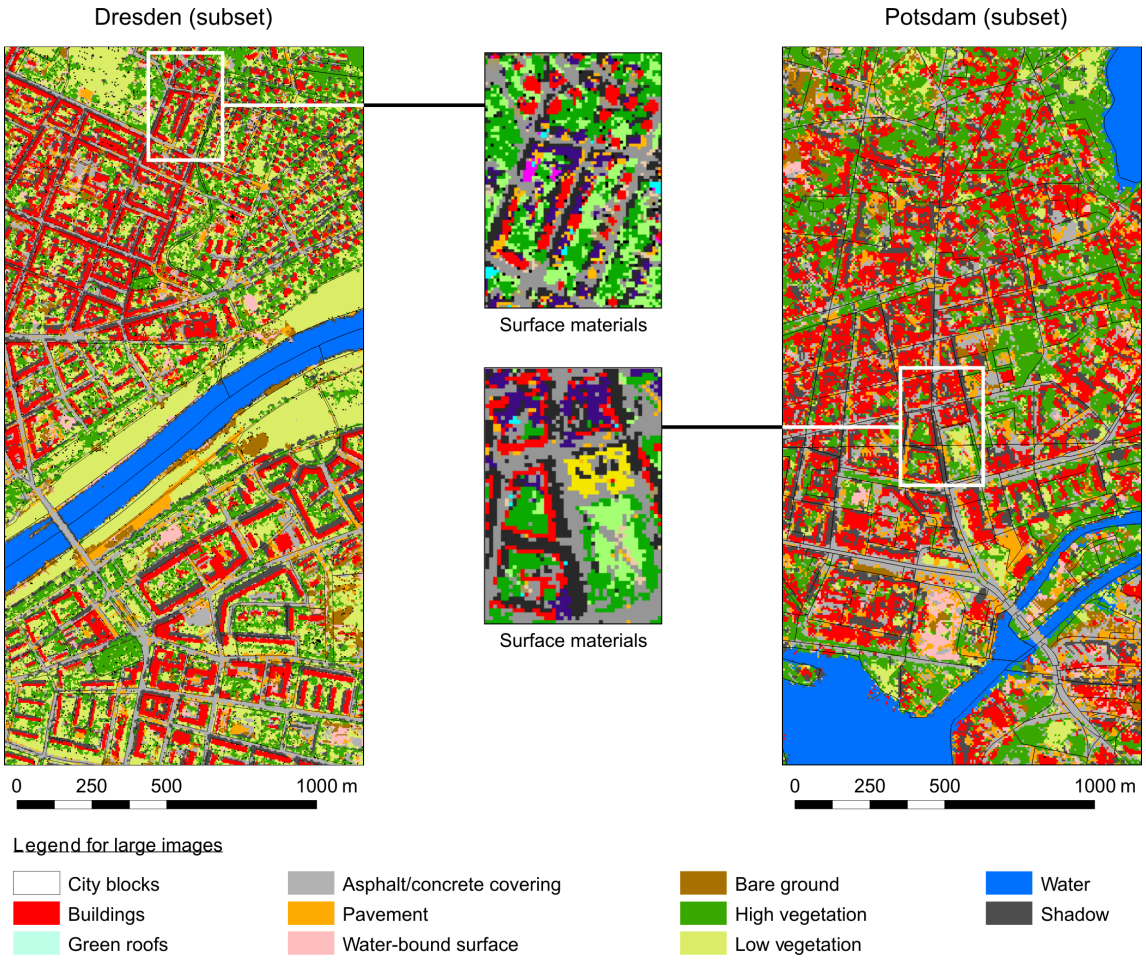

Figure 8: Linking categories derived from hyperspectral urban surface material classification based on the 2004 HyMap data of Dresden (left) and 1999 HyMap data of Potsdam (right). The insets show the original variety of urban surface materials (see Figure 5 for legend).

The definition of these weighting factors and the introduction of spatial mapping units (e.g., land parcels, urban biotopes, city blocks, districts or other administrative units) allow the automated calculation of urban ecological indicator values as well as the areal percentage of linking categories and surface materials for all spatial mapping units (Figure 6). The spatial mapping units and weighting factors can be defined by the user, which enables spatially and thematically flexible indicator calculation for the whole area of interest. The results, in the form of quantitative indicator values, can be used for further GIS-based analysis and cartographic visualisation supporting the objective ecological evaluation of urban areas.

Table 4: Indicator-specific weighting factors of linking categories ranging between 0 and 1, with the exception of the factor 'height' required for the indicators VVV and BV, and weighted by the object height in meters (m).

Linking categories	IMP	wIMP	OSV	OSIMP	wOSIMP	RC	IV	VDV	VCV	CCV	VVV	ESS1[c]	ESS2[c]	ESS3[c]	ESS4[c]	ESS5[c]	ESS6[c]	ESS7[c]	BD	BV
Buildings	1	1	0	-	-	1	0	0	0	0	0	0	0	0	0	0	0	0.1	1	height
Green roofs	1	1	0	-	-	0.4[a]	0	0	0	0	0.1 m[b]	1	0.2	0	0	0	0.2	0.5	1	height
Asphalt/concrete	1	0.9	1	1	0.9	0.9	0	0	0	0	0	0	0	0	0.1	0	0.1	0.1	0	0
Pavement	1	0.7	1	1	0.7	0.7[a]	0	0	0	0	0	0.2	0.1	0.3	0.3	0.4	0.5	0.3	0	0
Water-bound-surface	1	0.4	1	1	0.4	0.5[b]	0	0	0	0	0	0.3	0.1	0.4	0.6	0.8	0.5	0.4	0	0
Pool	1	1[b]	1	1	1[b]	0[b]	0	0	0	0	0	1	1	0	0	0	0	0	0	0
Pond	1	1[b]	1	1	1[b]	0[b]	0	0	0	0	0	1	1	0	0	0	0	0.6	0	0
Natural Water	0	0	1	0	0	0[b]	1	0	0	0	0	1	1	0[b]	1	1	1	1	0	0
Bare Ground	0	0	1	0	0	0[b]	1	0	0	0	0	0.3	0.1	0.5	1	1	1	0.5	0	0
High Vegetation	0	0	1	0	0	0[b]	1	1	0	1	height	0.8	0.8	0.8	1	0.4	0.9	0.9	0	0
Low Vegetation	0	0	1	0	0	0[b]	1	1	1	0	0.1 m	1	0.3	0.8	0.9	0.5	0.9	0.8	0	0
Shadow no veg.[d]	[0.1]	[0;0.9]	1	[0;1]	[0;0.9]	[0;0.9]	[0.1]	0	0	0	0	[0;0.3]	[0;0.1]	[0;0.5]	[0.1;1]	[0.1]	[0.1;1]	[0.1;0.5]	0	0
Shadow on veg.	0	0	1	0	0	0	1	1	1	0	0.1 m	1	0.3	0.8	0.9	0.5	0.9	0.8	0	0

[a] Average of multiple surface types considered in the original publication of the indicator. [b] New value not given in the original publication of the indicator. [c] The IEV is a complex indicator integrating seven ecosystem services (ESS): ESS1 (climatic regulation), ESS2 (dust settlement), ESS3 (retention of contaminants), ESS4 (surface porosity/permeability), ESS5 (groundwater recharge), ESS6 (infiltration of rainwater), and ESS7 (habitat formation). [d] Weighting factors within the given range are calculated automatically for each study area (see Section 3.3).

4. RESULTS OF URBAN ECOLOGICAL INDICATOR DERIVATION

4.1 Mapping of urban ecological indicators

Using the developed approach, a spatially continuous derivation of urban ecological indicators was performed by the direct calculation of individual urban ecological indicator values for each city block within the test sites of Dresden and Potsdam. In Figure 9, the results for three exemplary urban ecological indicators - *vegetation density value* (VDV), *imperviousness* (IMP) and *integrated ecological value* (IEV) - are depicted for one by one kilometre subsets of the two test sites. In both cases, the subsets cover parts of the respective city centres and adjacent areas. In Potsdam, the city centre is characterised by *vegetation density* values ranging between 0 and 30 % and *imperviousness* values larger than 70 %, while the other built-up areas vary between 10 and 80 % in *vegetation density* and between 30 and 90 % in *imperviousness*. In Dresden, the depicted part of the city centre is characterised by *vegetation density* values between 10 and 30 % and *imperviousness* values between 50 and 80 %. For the city park situated in the northern part of the subset, *imperviousness* values amount to approximately 10 % and *vegetation density* values to approximately 90 %. These results confirm the complementary character of the two analysed indicators.

In addition, the IEV has been calculated for the test site of Dresden. The IEV is a complex indicator integrating seven ecosystem services (ESS) such as climate regulation and groundwater recharge (Table 4). In contrast to other integrative indicators, it enables the evaluation and mapping of the individual ecosystem services separately in addition to its integrative value. Figure 9 shows the results of the IEV for the subset of the Dresden test site supplemented by the individual values for climatic regulation and groundwater recharge. The park in the north showing the highest *vegetation density* values is of high climatic importance (high values for ESS1), especially in regard to the adjacent highly overbuilt and impervious block development. This area is characterised by rather low *climatic regulation* values (ESS1) and low *groundwater recharge* values (ESS2), which are only slightly higher compared to the park area in the north due to the comparably high evapotranspiration rates of grass vegetation within the park.

The depicted exemplary results demonstrate the overall potential of the approach for ecological spatial differentiation, which can form the basis for further GIS-based analysis performed by experts responsible for urban planning. The selection and interpretation of implemented indicators can be adapted to the local needs of different cities and urban planning purposes.

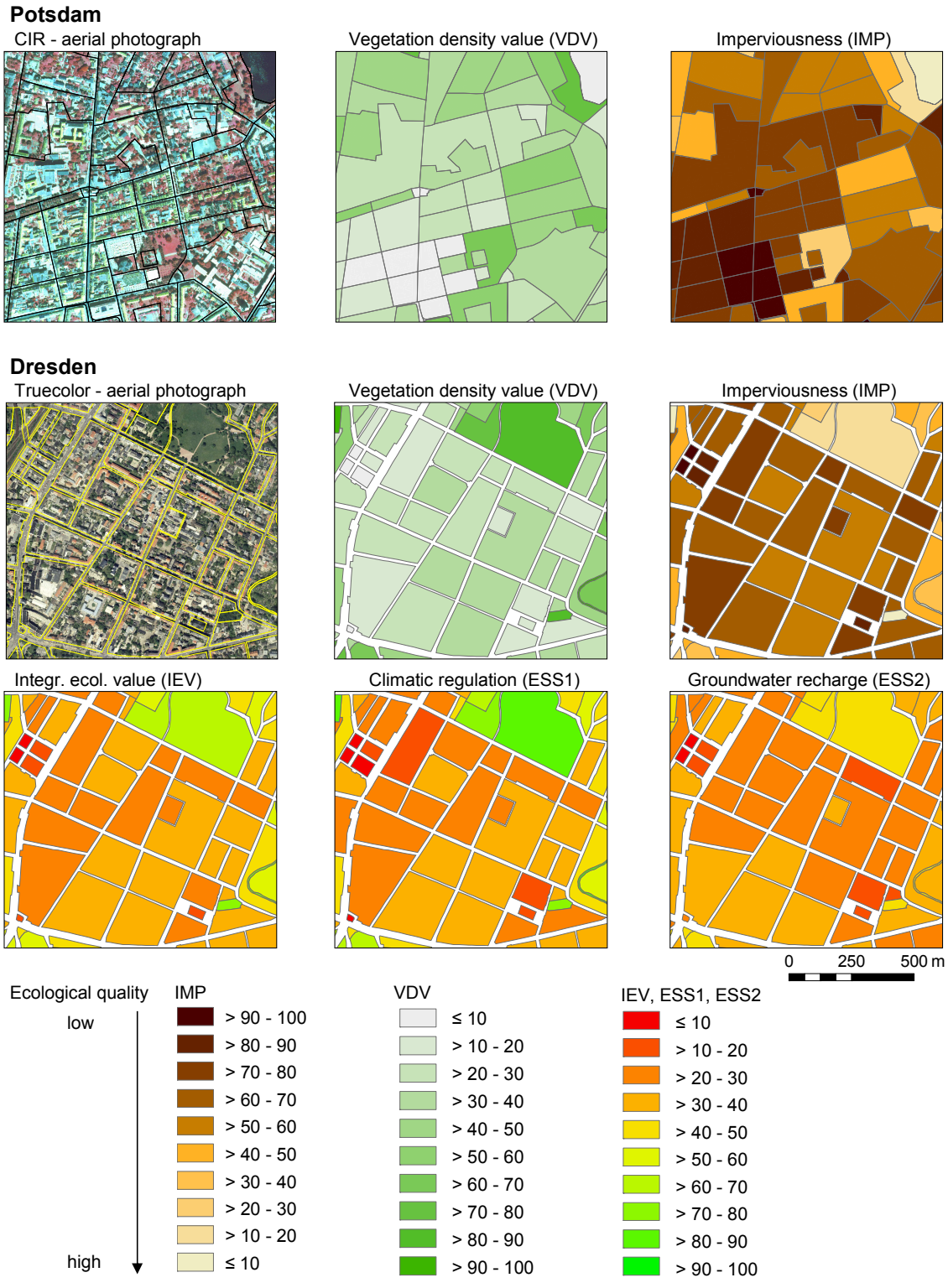

Figure 9: Aerial photographs and derived urban ecological indicators overlaid by city blocks as spatial mapping units for one by one kilometre subsets of the test sites of Dresden and Potsdam. Indicators: *vegetation density value* (VDV), *imperviousness* (IMP) and *integrated ecological value* (IEV), with two selected ecosystem services (ESS): climatic regulation and groundwater recharge (Table 4).

4.2 Accuracy assessment

For the accuracy assessment of the calculated urban ecological indicators, a total of 22 representative reference city blocks were mapped for the cities of Dresden and Potsdam based on aerial photographs and field surveys (Section 2.5). Accuracy assessments were conducted on the level of linking categories and on the level of indicators.

4.2.1 Accuracy assessment - Level of linking categories

A statistical accuracy assessment on the level of linking categories (Table 3) is presented in Figure 10, which depicts the mean areal coverage for each linking category calculated for the 22 reference city blocks of Dresden and Potsdam. A comparison between the areal proportions of the linking categories derived from hyperspectral image analysis and reference mapping shows that they are in good agreement with each other, with maximum differences of 4.7 % for asphalt/concrete covering and 4.4 % for low vegetation, whereas most of the linking categories are characterised by a slight underestimation. This is mainly due to areas classified as shadows amounting to an average of 12 % within the 22 reference blocks. Because shadows are predominantly cast over open spaces, these categories are subject to the highest differences. The occurrence of shadows can be minimised by choosing data acquisition times with high sun elevation. Moreover, discrimination between vegetated and non-vegetated shadowed areas can reduce the influence of shadows on the indicator values as described in Section 3.3.

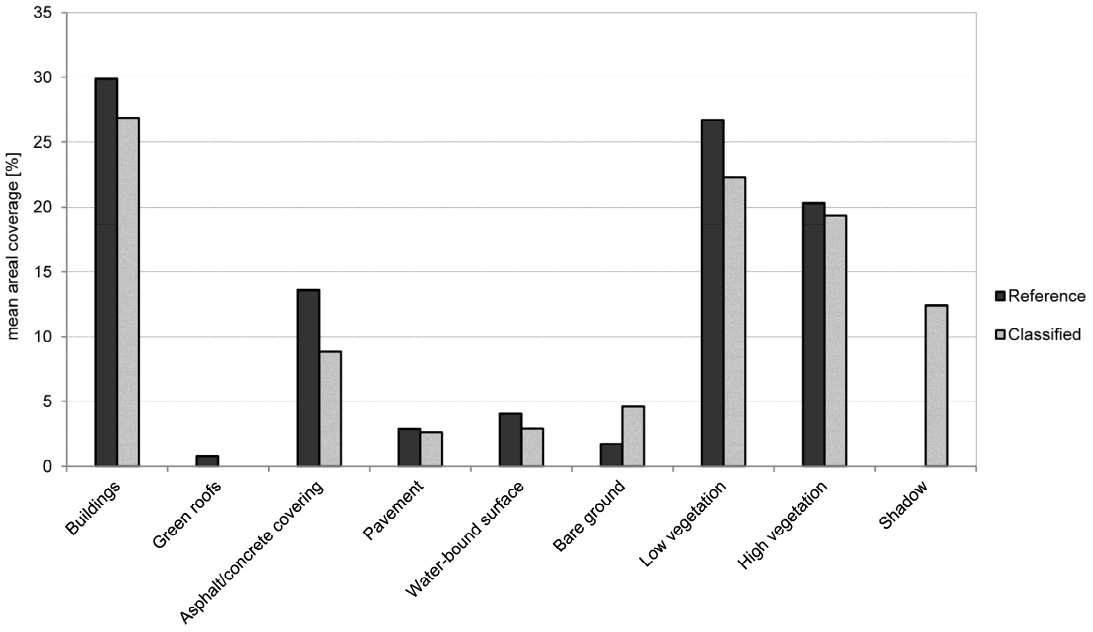

Figure 10: Mean areal coverage of linking categories derived by reference mapping (reference) and hyperspectral image analysis (classified) based on 22 representative city blocks for Dresden and Potsdam

4.2.2 Accuracy assessment - Level of indicators

For accuracy assessment on the indicator level, five urban ecological indicators (*imperviousness* (IMP), *runoff coefficient* (RC), *vegetation density value* (VDV), *building density* (BD), and *integrated ecological value* (IEV)) have been chosen to represent each ecological compartment and indicator type (Table 2). Accuracy statistics have been derived for each indicator based on the 22 reference city blocks. For this purpose, the differences

between indicator values calculated from hyperspectral image classification and those calculated from reference mapping have been analysed in form of the absolute error (AE; Figure 11a) and the relative error (E; Figure 11b), whereas the mean error values (MAE and ME) are depicted by the grey columns. The low mean absolute errors (MAE) of the indicators (approximately 4 %) demonstrate the suitability of the developed remote sensing-based approach. The mean relative errors (ME), indicating whether the remote sensing-based approach results in underestimation or overestimation, show a slight underestimation in comparison to the reference data for four out of the five indicators. This is caused by the already discussed underestimation of the linking categories used for indicator calculation (Figure 10). In contrast, the overestimation of the *integrated ecological value* (IEV) results from the inverse behaviour of the corresponding weighting factors of these linking categories with respect to the ecological quality (Figure 9).

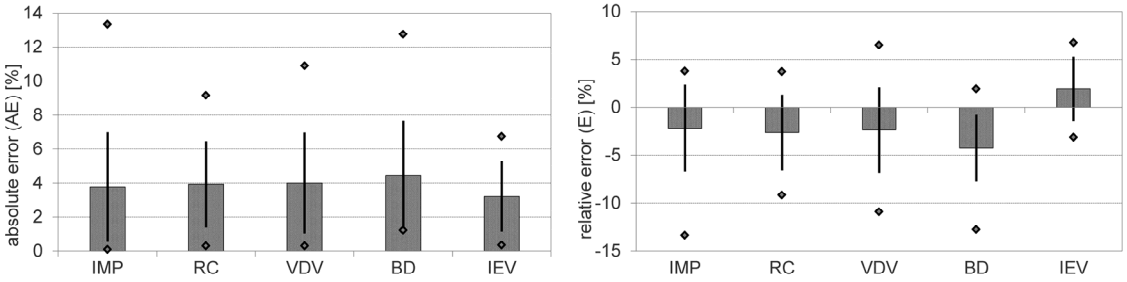

Figure 11: Accuracy of hyperspectral indicator derivation – comparison between absolute (a) and relative (b) errors. Mean errors are depicted by grey columns, standard deviations by solid lines, and minimum and maximum error values by dots. Indicator abbreviations are explained in Table 2.

4.3 Comparison with results from visual indicator estimation

For the *imperviousness* (IMP) indicator, the accuracy of remote sensing based indicator values (Section 4.2) has also been compared to the accuracy of indicator values derived by the visual estimation method, which are contained in the USU dataset provided by the municipality of Dresden (Section 2.4). Table 5 shows the comparison between the visually estimated values (IMP_{VIS}) and the ones derived by hyperspectral remote sensing (IMP_{HY}) along with the values calculated for each of the manually digitised reference blocks (IMP_{REF}). For only 7 out of 19 city blocks (37 %) the reference indicator values fall into the class of the visual estimation method (IMP_{REF} in IMP_{VIS}). In all of the remaining 12 blocks, the visually estimated classes represent an overestimation of *imperviousness* in comparison to the values obtained from the reference dataset. In contrast, the remote sensing-based indicator values differ less than 10 % from the reference indicator values (IMP difference), except for one outlier (city block no. 16). Classifying the remote sensing-based results in the same 20 %-step classes, which have been used for visual estimation, conformity of 95 % (18 of 19 city blocks) has been achieved (IMP_{HY} in IMP_{REF} +/-10). These results clearly show the superiority of the objective automated remote sensing-based approach in comparison to the visual estimation method, which is characterised by a high degree of subjectivity.

Table 5: Comparison of *imperviousness* (IMP) values in % derived by the hyperspectral approach (IMP_{HY}) and by the visual estimation method (IMP_{VIS} - contained in USU data set of Dresden) for the 19 reference mapping blocks of Dresden. IMP_{REF} in IMP_{VIS}: 20 % IMP_{VIS} class correctly contains the reference imperviousness values (IMP_{REF}); IMP_{HY} in IMP_{REF} +/-10: IMP_{HY} falls within a corresponding +/- 10 % class of IMP_{REF}, simulating the same 20 % scale; • Value falls in the 20 %-step class

No.	Area [m²]	IMP_{REF} *reference mapping*	IMP_{HY} *hyperspectral approach*	IMP difference *IMP_{REF} - IMP_{HY}*	IMP_{VIS} *visual estimation class USU dataset Dresden*	IMP_{REF} in IMP_{VIS}	IMP_{HY} in IMP_{REF} +/-10
1	16571	31	27	-4	40-60		•
2	27911	33	30	-3	40-60		•
3	27756	34	28	-6	40-60		•
4	8975	42	45	3	40-60	•	•
5	13264	42	37	-5	40-60	•	•
6	21976	42	41	-1	40-60	•	•
7	26953	46	43	-3	40-60	•	•
8	10840	42	42	0	60-80		•
9	18135	44	39	-5	60-80		•
10	24186	48	47	-1	60-80		•
11	14341	48	39	-9	60-80		•
12	10197	55	55	0	60-80		•
13	54453	57	60	3	60-80		•
14	30684	58	59	1	60-80		•
15	28047	61	55	-6	60-80	•	•
16	12969	66	53	-13	60-80	•	
17	6846	73	75	2	80-100		•
18	13588	74	76	2	80-100		•
19	7867	80	84	4	80-100	•	•

5. DISCUSSION

The developed remote sensing and GIS-based system for the flexible and efficient calculation of ecological indicators is based on automated surface material mapping using airborne hyperspectral image data and height information. As a result, fractional abundance layers are obtained for a large variety of urban surface materials. In the second step, the surface material classes have been transformed into linking categories representing the surface types that are needed within the developed GIS-based system for flexible indicator calculation (Section 3.3). Based on these linking categories, 14 urban ecological indicators have been implemented in the GIS-based system, enabling their automated and reproducible calculation in a spatially continuous way. They comprise (non-)weighted parameters and integrated ecological indicators (Table 2). For 11 of these indicators, the required surface types could be completely derived from the hyperspectral material mapping results. Slight modifications only needed to be applied to three of the original indicators (RC, VVV and IEV) to facilitate their GIS-based calculation. These results show that automated hyperspectral material mapping is capable of providing suitable input information for subsequent GIS-based indicator derivation.

However, the comprehensive remote sensing-based assessment of surface types needed for ecological indicator derivation requires the integration of additional object height information into the automated material mapping approach to distinguish between spectrally similar materials representing different surface types. This is especially important for discriminating between buildings and open surfaces of similar material coverage. Such height information is also needed to differentiate between low, mid-height and high vegetation (Table 4). For this purpose, a LiDAR-based DSM is needed that contains height information for the ground and vegetation top levels. However, the available LiDAR dataset is not suitable for a reliable differentiation between vegetation heights, because it had been acquired outside of the growing season. However, it has been possible to distinguish between high (trees) and low (meadow, lawn) vegetation solely based on spectral characteristics. The future wide availability of high quality object height information, such as detailed 3D city models, will further increase the reliability of automated surface type mapping.

Another principle problem for all remote sensing-based methods is the presence of shadows in the image data. In the case of the analysed test sites, the shadowed areas amount to approx. 13 %. To reduce the influence of shadows on the calculation of indicator values, the differentiation between shadows on vegetated and non-vegetated surfaces and the derivation of indicator- and area-specific weighting factors for the two shadow classes (Section 3.3) has been implemented. The influence of shadows can be further reduced by choosing data acquisition times with high sun elevation.

For accuracy assessment, five representative urban ecological indicators were selected and indicator values were calculated for the 22 reference city blocks (Section 4.2). Overall, the mean absolute error (MAE) amounts to approximately 4 % for all five indicators, whereas the maximum absolute errors for the individual indicators range between 7 % and 14 %. These small errors demonstrate the general suitability of the developed remote sensing-based approach for automated indicator calculation for large areas. These results were also compared to the results obtained by the visual estimation approach (Section 4.3), representing one of the state-of-the-art methods used for ecological indicator derivation in urban planning practice. Visually estimated *imperviousness* values have been compared to the ones calculated from the reference mapping. This comparison has revealed that only for a minority of city blocks (7 out of 19) could the same class membership be achieved. In contrast, grouping the indicator values obtained by the developed automated approach into the same discrete categories has resulted in conformity of 95 % (18 out of 19 city blocks). These results demonstrate the superiority of the developed approach with regard to reliability and efficiency. Moreover, the approach also distinguishes itself by its objective reproducibility.

The accuracies of the developed direct approach are also compared to the accuracies that, in principle, can be achieved by the urban structural units (USU) based extrapolation approach (Section 1). Because this approach assumes a single characteristic indicator value for all mapping units belonging to the same USU, the real variability of indicator values occurring between these mapping units has to be assessed to evaluate the achievable accuracy. For this purpose, Pauleit and Duhme (2000) have analysed the *imperviousness* (IMP) and *vegetation density value* (VDV) of 621 mapping units belonging to USUs of different residential types, whereas the indicator values for the individual mapping units were determined by visual estimation. The results show considerably high standard deviations within the same USUs ranging between 14.8 % and 18.1 %, which

significantly exceeds the uncertainty related to the developed approach (MAE of approximately 4 %). Heiden et al. (2012) have analysed the variability of the same indicators for 664 mapping units belonging to similar USU types. In comparison to Pauleit and Duhme (2000), they observed significantly lower standard deviations ranging between 5 % and 11 %. This difference might be attributed to the mapping methods used – which in the case of Heiden et al. (2012) is based on hyperspectral image analysis and height information – or to the determination of USU-types, which often differs between cities. These results confirm that the accuracies of indicator calculations obtained by the developed approach are sufficient to resolve the existing variability of indicator values occurring between the different mapping units of the same USU.

The use of hyperspectral remote sensing data also allows regular updates of the information base, whereas the objectivity and long-term stability of the analysis are ensured by the physically based automated mapping of the underlying urban surface materials. Thus, the developed GIS-based system can be applied to all urban areas of comparable surface material coverage. This principle methodological transferability has been shown by applying the approach to the two test sites within the German cities of Dresden and Potsdam. Urban areas outside of Mid-European cities may comprise additional surface materials. In such cases, the developed approach can be extended by integrating the spectral reflectance signatures of additional materials into the automated hyperspectral mapping process, which may also require the determination of new linking categories for transforming material classes into ecologically relevant surface types. Due to the developed graphical user interface, the GIS-based system can be adapted to the different local conditions as long as hyperspectral remote sensing data of sufficient spatial resolution higher than 10 m (Weng, 2012) are available.

6. CONCLUSIONS AND OUTLOOK

A new automated remote sensing and GIS-based system has been developed for the flexible calculation of user-defined urban indicators, which significantly reduces the mapping effort by computer-based processing and automation for large parts of the procedure. This system comprises the variable determination of mapping units, surface material types and respective weighting factors, and the implementation of additional user-defined indicators accommodating a large variety of user needs and urban conditions. Moreover, the developed system allows the objective and reproducible calculation of indicator values as a result of the computer-based automation. In contrast, most state-of-the-art methods comprise a large amount of manual effort and thus are likely to be biased by the subjectivity of the analyst. Because the developed system is characterised by objectivity, automation and flexibility, it enables the efficient analysis of large areas, the calculation of a variety of ecological indicators using the same information base, the accommodation of various user needs and local conditions. This way, the developed system opens up new opportunities for a wider use of urban ecological indicators in the urban planning practice.

Such a broad application, including the possible operational use of the developed system, highly depends on the availability of suitable hyperspectral remote sensing data, which has continuously improved over the previous years due to the increasing number of available airborne hyperspectral systems (e.g., CASI, HyMap, AISA, HySpex, and APEX). Further opportunities will open up with the launch of new hyperspectral (EnMAP) and superspectral (Sentinel-2, WorldView-3) satellite systems acquiring data with increased spectral resolution. However, the limited spatial resolution of the EnMAP (30 m) and the Sentinel-2 (10 –20 m) satellite-based

systems will require the development of new data fusion methods, allowing their combined use with optical and radar satellite remote sensing data of higher spatial resolution. In this context, the WorldView-3 superspectral satellite system, covering the VNIR-SWIR spectral range with 16 bands at a spatial resolution of at least 3.7 m, has big potential for urban analysis, whereas the capabilities of the SWIR bands are of special interest for the improved differentiation of non-vegetated areas. The developed system for the calculation of urban ecological indicators can be adapted to the use of such operationally acquired satellite remote sensing data, which will enlarge its potential applicability to a worldwide scale and thus increase the opportunities for regular monitoring and updates. This is especially important for managing the development of large urban agglomerations, representing a rapidly growing global phenomenon.

ACKNOWLEDGEMENTS

The authors would like to thank the anonymous reviewers for their valuable comments and suggestions that substantially contributed to clarifying and improving the paper. The presented work was supported by the Helmholtz Integrated Earth Observing System (EOS) PhD program. Hyperspectral image data were recorded during HyMap flight campaigns carried out by the DLR between 1999 and 2007. We also thank the municipality of Potsdam for providing the ATKIS DLM 25 data and the Municipal Environmental Agency of Dresden for providing the urban structural unit data set and the Laser DSM

REFERENCES

Arlt, G., Lehmann, I., 2005. Ökologische Flächenleistungen - Methodische Grundlagen; Analyse und Bewertung teilstädtischer Gebiete in Dresden. IOER, Dresden.

Banzhaf, E., Höfer, R., 2008. Monitoring urban structure types as spatial indicators with CIR aerial photographs for a more effective urban environmental management. IEEE J. Sel. Top. Appl. Earth Obs. Remote Sens. 1, 129-138.

Bateson, A., Asner, G.P., Wessman, C.A., 2000. Endmember bundles: A new approach to incorporating endmember variability into spectral mixture analysis. IEEE TGARS 38, 1083-1094.

Berlekamp, L.R., Pranzas, N., 1986. Methode zur Erfassung der Bodenversiegelung von städtischen Wohngebieten. Natur & Landschaft 61, 92-95.

Berlekamp, L.R., Pranzas, N., 1992. Erfassung und Bewertung von Bodenversiegelung unter hydrologisch-stadtplanerischen Aspekten am Beispiel eines Teilraums von Hamburg. Univ. Hamburg.

Blaschke, T., Hay, G.J., Weng, Q., Resch, B., 2011. Collective Sensing: Integrating Geospatial Technologies to Understand Urban Systems-An Overview. Remote Sens. 3, 1743–1776.

Bochow, M., 2010. Automatisierungspotenzial von Stadtbiotopkartierungen durch Methoden der Fernerkundung, Fachbereich Mathematik/Informatik. Universität Osnabrück, Osnabrück, p. 189.

Bochow, M., Peisker, T., Roessner, S., Segl, K., Kaufmann, H., 2010. Towards an automated update of urban biotope maps using remote sensing data: What is possible?, In: Müller, N., Werner, P., Kelcey, J.G. (Eds.), Urban biodiversity and design. Wiley-Blackwell, Oxford, pp. 255-272.

Böhm, P., 1998. Urban Structural Units as a Key Indicator for Monitoring and Optimising the Urban environment, in: Breuste, J., Feldmann, H., Uhlmann, O. (Eds.), Urban Ecology. Springer, Berlin, pp. 442-445.

Bolund, P., Hunhammar, S., 1999. Ecosystem services in urban areas. Ecol. Econ. 29, 293–301.

Bötticher, M., Fisch, R., 1988. Zur Einführung des Biotopflächenfaktors (BFF) in die Landschafts-und Bauleitplanung. Das Gartenamt, Jg 37.

Bunzel, A., 1992. Begrenzung der Bodenversiegelung: Planungsziele und Instrumente. Deutsches Institut für Urbanistik.

Button, K., 2002. City management and urban environmental indicators. Ecol. Econ. 40, 217–233.

Cabral, P., 2007. Delineation of urban areas from a Landsat ETM+ image: comparison of classification methods. Can. J. Remote Sens. 33, 422-430.

Cadenasso, M.L., Pickett, S.T.A., Schwarz, K., 2007. Spatial heterogeneity in urban ecosystems: reconceptualizing land cover and a framework for classification. Front. Ecol. Environ. 5, 80-88.

Carlson, T.N., 2004. Analysis and Prediction of Surface Runoff in an Urbanizing Watershed Using Satellite Imagery. J. Am. Water Resour. Assoc. 40, 1087–1098.

Carmona, M., Heath, T., Oc, T., Tiesdell, S., 2003. Public Places - Urban Spaces. The Dimensions of Urban Design: A Guide to Urban Design. Architectural Press.

Cocks, T., Jenssen, R., Stewart, A., Wilson, I., Shields, T., 1998. The HyMap TM airborne hyperspectral sensor: the system, calibration and performance, 1st EARSeL Workshop on Imaging Spectroscopy, Zürich, pp. 37-42.

Dennison, P.E., Roberts, D.A., 2003. Endmember selection for multiple endmember spectral mixture analysis using endmember average RMSE. Remote Sens. Environ. 87, 123-135.

Din, 1995. Entwässerungsanlagen für Gebäude und Grundstücke - Ermittlung der Nennweiten von Abwasser- und Lüftungsleitungen. Beuth Verlag, Berlin.

Eliasson, I., Svensson, M.K., 2003. Spatial air temperature variations and urban land use - a statistical approach. Meteorol Appl 10, 135-149.

Fauvel, M., Benediktsson, J.A., Chanussot, J., Sveinsson, J.R., 2008. "Spectral and Spatial Classification of Hyperspectral Data Using SVMs and Morphological Profiles." IEEE TGARS 46 (11): 3804–14.

Franke, J., Roberts, D.A., Halligan, K., Menz, G., 2009. Hierarchical Multiple Endmember Spectral Mixture Analysis (MESMA) of hyperspectral imagery for urban environments. Remote Sens. Environ. 113, 1712–1723.

Frick, A., 2006. Urban monitoring with Quickbird imagery through a knowledge-based extraction of indices, ISPRS Workshop - Fifth International Symposium, Turkish German Joint Geodetic days, Berlin.

Gao, F., de Colstoun, E.B., Ma, R., Weng, Q., Masek, J.G., Chen, J., Pan, Y., Song, C., 2012. Mapping impervious surface expansion using medium-resolution satellite image time series: a case study in the Yangtze River Delta, China. Int. J. Remote Sens. 33, 7609–7628.

Gill, S.E., Handley, J.F., Ennos, A.R., Pauleit, S., Theuray, N., Lindley, S.J., 2008. Characterising the urban environment of UK cities and towns: A template for landscape planning. Landsc. Urban Plan. 87, 210-222.

Goetz, A.F.H., 2009. Three decades of hyperspectral remote sensing of the Earth - A personal view. Remote Sens. Environ. 113, S5-S16.

Gomarasca, M.A., Brivio, P.A., Pagnoni, F., Galli, A., 1993. One Century of Land-Use Changes in the Metropolitan-Area of Milan (Italy). Int. J. Remote Sens.14, 211-223.

Gómez, F., Jabaloyes, J., Montero, L., De Vicente, V., Valcuende, M., 2011. Green Areas, the Most Significant Indicator of the Sustainability of Cities: Research on Their Utility for Urban Planning. J. Urban Plan. Dev. 137, 311–328.

Gomez-Baggethun, E., Barton, D.N., 2013. Classifying and valuing ecosystem services for urban planning. Ecol. Econ. 86, 235–245.

Gupta, K., Kumar, P., Pathan, S.K., Sharma, K.P., 2012. Urban Neighborhood Green Index - A measure of green spaces in urban areas. Landsc. Urban Plan. 105, 325–335.

Haggag, M.A., Ayad, H.M., 2002. The urban structural units method: a basis for evaluating environmental prospects for sustainable development. Urban Des. Int. 7, 97-108.

Haid, N., Treter, U., 2004. Die Bodenversiegelung in Erlangen: Bestandsaufnahme und Bewertung. Mitteilungen der Fränkischen Geographischen Gesellschaft 50/51, 115-126.

Heber, B., Lehmann, I., 1996. Beschreibung und Bewertung der Bodenversiegelung in Städten. IÖR, Dresden.

Hecht, R., Meinel, G., Buchroithner, M.F., 2008. Estimation of Urban Green Volume Based on Single-Pulse LiDAR Data. IEEE TGARS. 46, 3832–3840.

Heiden, U., Heldens, W., Roessner, S., Segl, K., Esch, T., Mueller, A., 2012. Urban structure type characterization using hyperspectral remote sensing and height information. Landsc. Urban Plan. 105, 361-375.

Heiden, U., Segl, K., Roessner, S., Kaufmann, H., 2007. Determination of robust spectral features for identification of urban surface materials in hyperspectral remote sensing data. Remote Sens. Environ. 111, 537-552.

Heldens, W., Heiden, U., Esch, T., Stein, E., Muller, A., 2011. Can the Future EnMAP Mission Contribute to Urban Applications? A Literature Survey. Remote Sens. 3, 1817–1846.

Henry, J.A., Dicks, S.E., 1987. Association of urban temperature with land use and surface materials. Landsc. Urban Plan. 14, 21–29.

Hepner, G.F., Chen, J., 2001. Investigation of imaging spectroscopy for discriminating urban land cover and surface materials, AVIRIS Earth Science and Applications Workshop, Palo Alto, CA.

Herold, M., Gardner, M.E., Roberts, D.A., 2003. Spectral resolution requirements for mapping urban areas. IEEE TGARS 41, 1907-1919.

Herold, M., Roberts, D.A., Gardner, M.E., Dennison, P.E., 2004. Spectrometry for urban area remote sensing - Development and analysis of a spectral library from 350 to 2400 nm. Remote Sens. Environ.91, 304-319.

Illgen, M., 2000. Überprüfung von Standard-Abflussbeiwerten durch Niederschlag-Abfluss-Simulation. Universität Kaiserslautern.

Jat, M.K., Garg, P.K., Khare, D., 2008. Monitoring and modelling of urban sprawl using remote sensing and GIS techniques. Int. J. Appl. Earth Obs. Geoinf. 10, 26-43.

Kim, H.-O., Kenneweg, H., Kleinschmit, B., 2006. A new approach towards mapping urban sealing using the very high-resolution satellite data in Seoul metropolitan areas, in: 1 St EARSel Workshop of the SIG Urban Remote Sensing, HU Berlin. pp. 2–7

Komossa, S., Meyer, H., Risselada, M., Thomaes, S., 2005. Atlas of the dutch urban block. Thoth Uitgeverij.

Kraus, K., Pfeifer, N., 2001. Advanced DTM generation from LIDAR data, WGIII/3-6 Workshop "Land surface mapping and characterization using laser altimetry", Annapolis, Maryland, pp. 23-30.

Krause, K.H., 1989. Zur Erfassung der Oberflächenarten für eine stadtökologische Zustandsbeschreibung. Hallesches Jahrbuch für Geowissenschaften 14, 124-130.

Kumar, A., Pandey, A.C., Jeyaseelan, A.T., 2012. Built-up and vegetation extraction and density mapping using WorldView-II. Geocarto Int. 27, 557–568.

Lakes, T., Kim, H.-O., 2012. The urban environmental indicator “Biotope Area Ratio”—An enhanced approach to assess and manage the urban ecosystem services using high resolution remote-sensing. Ecol. Indic. 13, 93-103.

Li, F., Liu, X.S., Hu, D., Wang, R.S., Yang, W.R., Li, D., Zhao, D., 2009. Measurement indicators and an evaluation approach for assessing urban sustainable development: A case study for China’s Jining City. Landsc. Urban Plan. 90, 134–142.

Li, X., Zhou, W., Ouyang, Z., Xu, W., Zheng, H., 2012. Spatial pattern of greenspace affects land surface temperature: evidence from the heavily urbanized Beijing metropolitan area, China. Landsc. Ecol. 27, 887–898.

Lo, C.P., 1997. Application of Landsat TM data for quality of life assessment in an urban environment. Comput. Environ. Urban Syst. 21, 259-276.

Lu, D.S., Weng, Q.H., 2004. Spectral mixture analysis of the urban landscape in Indianapolis with landsat ETM plus imagery. Photogramm. Eng. Remote Sens. 70, 1053-1062.

Mayer, S., 2000. Retrieving object borders and height from high-resolution digital surface models, World Multiconference on Systems, Cybernetics and Informatics, Orlando, FL, USA, pp. 433-438.

Munier, N., 2011. Methodology to select a set of urban sustainability indicators to measure the state of the city, and performance assessment. Ecol. Indic. 11, 1020–1026.

Pauleit, S., Duhme, F., 2000. Assessing the environmental performance of land cover types for urban planning. Landsc. Urban Plan. 52, 1-20.

Pickett, S.T.A., Cadenasso, M.L., Grove, J.M., Nilon, C.H., Pouyat, R.V., Zipperer, W.C., Costanza, R., 2001. Urban ecological systems: Linking Terrestrial Ecological, Physical, and Socioeconomic Components of Metropolitan Areas. Annual Review of Ecology and Systematics 32, 127-157.

Plaza, A., Benediktsson, J.A., Boardman, J.W., Brazile, J., Bruzzone, L., Camps-Valls, G., Chanussot J., et al. 2009. "Recent Advances in Techniques for Hyperspectral Image Processing." Remote Sens. Environ.113, Supplement 1 (September). Imaging Spectroscopy Special Issue: S110–S122.

Pohl, W., 1991. Werte für die Landschafts-und Bauleitplanung, Bodenfunktionszahl - Grünvolumenzahl. Mitt. NNA-Mitteilungen 4, 2-6.

Richter, R., Schläpfer, D., 2002: Geo-atmospheric processing of airborne imaging spectrometry data. Part 2: Atmospheric/Topographic Correction. Int. J. Remote Sens., 23(13), 2631-2649.

Roessner, S., Segl, K., Bochow, M., Heiden, U., Heldens, W., Kaufmann, H., 2011. Potential of hyperspectral remote sensing for analyzing the urban environment, in: Yang, X. (Ed.), Urban Remote Sensing: Monitoring, Synthesis and Modeling in the Urban Environment. Wiley, Oxford, pp. 49-62.

Roessner, S., Segl, K., Heiden, U., Kaufmann, 2001. Automated differentiation of urban surface based on airborne hyperspectral imagery. IEEE TGARS 39, 1523-1532.

Rose, H., 1991. Der KÖP-Wert in der ökologisch orientierten Stadtplanung - Zur Bewertung umweltrelevanter Faktoren im Rahmen der kommunalen Umweltverträglichkeitsprüfung. Im Selbstverlag des Geographischen Instituts der Universität Mannheim, Mannheim.

Sandtner, M., 1998. Die Erfassung von staedtischen Oberflaechen mittels EDV-gestuetzter Luftbildauswertung. Geogr. Helv. 53, 69-76.

Schiller, G., 2003. The urban structure unit approach - a suitable frame for environmental and spatial urban investigations, 8th International Conference on Environmental Science and Technology, Lemnos Island, Greece.

Schläpfer, D., Richter, R., 2002: Geo-atmospheric Processing of Airborne Imaging Spectrometry Data Part 1: Parametric Orthorectification. Int. J. Remote Sens., 23(13), 2609-2630.

Schöpfer, E., Lang, S., Blaschke, T., 2005. A "green index" incorporating remote sensing and citizen's perception of green space. Int. Arch. Photogramm Remote Sens. Spat. Inf. Sci. 1–6.

Schulte, W., Sukopp, H., Werner (eds.), P., Arbeitsgruppe "Methodik der Biotopkartierung im besiedelten Bereich", 1993. Flächendeckende Biotopkartierung im besiedelten Bereich als Grundlage einer am Naturschutz orientierten Planung - Programm für die Bestandsaufnahme, Gliederung und Bewertung des besiedelten Bereichs und dessen Randzonen. Natur und Landschaft 68, 491-526.

Schulz, A., 1982. Der KÖH-Wert, Modell einer komplexen, planungsrelevanten Zustandserfassung. Inform. z. Raumentwicklung 10, 847-863.

Schulze, H.D., Pohl, W., Großmann, M., 1984. Werte für die Landschafts- und Bauleitplanung - Bodenfunktionszahl, Grünvolumenzahl, Grünzahl. Hamburg / Behörde für Bezirksangelegenheiten, Naturschutz und Umweltgestaltung, Hamburg.

Schwarz, N., 2010. Urban form revisited—Selecting indicators for characterising European cities. Landsc. Urban Plan. 96, 29–47.

Segl, K., Roessner, S., Heiden, U., Kaufmann, H., 2003. Fusion of spectral and shape features for identification of urban surface cover types using reflective and thermal hyperspectral data. ISPRS-J. Photogramm. Remote Sens. 58, 99-112.

Theseira, M.A., Thomas, G., Taylor, J.C., Gemmell, F., Varjo, J., 2003. Sensitivity of mixture modelling to end-member selection. Int. J. Remote Sens. 24, 1559-1575.

Towers, G., 2005. An Introduction to Urban Housing Design: At Home in the City. Architectural Press.

Tuia, D., Camps-Valls, G., 2011. Urban Image Classification With Semisupervised Multiscale Cluster Kernels. IEEE J. Sel. Top. Appl. Earth Obs. Remote Sens. 4, 65–74.

van der Meer, F.D., de Jong, S.M., 2001. Imaging spectrometry - Basic principles and prospective applications. Kluwer Academic Publishers.

Weng, Q.H., Rajasekar, U., Hu, X.F., 2011. Modeling Urban Heat Islands and Their Relationship With Impervious Surface and Vegetation Abundance by Using ASTER Images. IEEE TGARS 49, 4080–4089.

Weng, Q.H., 2012. Remote sensing of impervious surfaces in the urban areas: Requirements, methods, and trends. Remote Sens. Environ. 117, 34–49.

Yuan F., Wu, C., Bauer, M.E., 2008. Comparison of spectral analysis techniques for impervious surface estimation using Landsat imagery. Photogramm. Eng. Remote Sens. 74, 1045–1055.